Battery-Buffered Alkaline Water Electrolysis Powered by Photovoltaics

Maik Becker[1,2,*], Jörn Brauns[1], and Thomas Turek[1,2]

DOI: 10.1002/cite.202000151

Supporting Information available online

The combination of an alkaline water electrolyzer (AWE) with a battery system powered by photovoltaics (PV) for the production of green hydrogen is investigated. A model describes the power distribution between these three subsystems (AWE, battery and PV). Variation of AWE and battery power and capacity is carried out for two locations, to identify the most appropriate setup, where the highest energy usage and operating time can be reached. The battery helps to reduce the power level of the AWE. However, an estimation of the costs indicates that further optimization is necessary.

Keywords: Battery, Energy storage, Green hydrogen, Photovoltaics, Water electrolysis

Received: July 16, 2020; *revised:* December 27, 2020; *accepted:* January 04, 2021

1 Introduction

The latest reports of the IPCC emphasize the urgent need to reduce greenhouse gas emissions rapidly to circumvent threatening scenarios of anthropogenic climate change [1]. Renewable energies such as photovoltaics (PV) and wind power play a crucial role in the transformation of the energy supply, which is currently responsible for a major part of global greenhouse gas emissions. However, the fluctuating nature of wind power and photovoltaics requires a buffering of their electrical energy output, for which batteries and water electrolysis can be an economic and ecologic solution. Batteries are mainly applied for short to medium term local energy storage of up to several hours but can achieve rather high efficiencies for accumulation and release of electrical energy. Water electrolysis reaches lower efficiencies if the input and output of electrical energy is considered. Nevertheless, hydrogen produced by water electrolysis enables a variety of routes, such as seasonal energy storage, conversion to methane, methanol, ammonia, and other valuable products that allow an already established transport of energy bound in chemical compounds. These opportunities have been recognized at political levels and resulted in several regional, national and international reports, initiatives and strategies focusing on the application and integration of hydrogen technologies [2–4].

Photovoltaic systems have been applied globally with a significant cost reduction in the last years and record low bids below 20 $ per MWh [5]. Wind power on the other hand, achieves lowest prices around 50 $ per MWh [6], sometimes even down to 20 $ per MWh [7]. The use of PV or wind power to supply a water electrolyzer producing green hydrogen could theoretically lead to hydrogen costs of 1.0 to 2.6 US $ kg^{-1} at an assumed efficiency of 75 % of the electrolysis process. Neglecting other costs (investment, operation) green hydrogen could therefore reach the range of costs of conventional hydrogen produced by steam reforming of methane (1.25 $ kg^{-1} to 3.50 $ kg^{-1}) [8]. Unfortunately, the water electrolysis system has to deal with the fluctuating power output of PV and wind power. Water electrolysis systems divide in two different technologies that are commercially available on a large scale: the alkaline water electrolysis (AWE) operating with mainly nickel electrodes in an alkaline electrolyte circulating through both half-cells and the polymer electrolyte membrane water electrolysis (PEM), where a proton-conducting membrane separates both half-cells with electrodes based on precious metals (Ir, Pt) [9, 10]. Both technologies can differentiate in terms of efficiency, power specific costs, dynamic response behavior, gas quality, operating pressure and ecological footprint and it is currently not clear which, if any, technology will dominate the future water electrolysis market.

[1]Dr.-Ing. Maik Becker, Jörn Brauns, Prof. Dr.-Ing. Thomas Turek
maik.becker@tu-clausthal.de
Clausthal University of Technology, Institute of Chemical and Electrochemical Process Engineering, Leibnizstraße 17, 38678 Clausthal-Zellerfeld, Germany.

[2]Dr.-Ing. Maik Becker, Prof. Dr.-Ing. Thomas Turek
Clausthal University of Technology, Research Center for Energy Storage Technologies, Am Stollen 19A, 38640 Goslar, Germany.

Water electrolysis powered by renewables is investigated in a couple of studies [11–18], however, only a few deal with the potential benefits of water electrolysis buffered by battery systems for hydrogen production. Gökcek et al. investigated and optimized a system of PV, wind power, electrolyzer, battery, hydrogen storage and compression for refueling 25 hydrogen vehicles per day using a techno-economical model [13]. The optimized system achieved hydrogen costs of 7.5 \$ kg^{-1} for battery costs as low as 110 \$ per kWh (lead acid batteries). Unfortunately, the electrolyzer used only slightly more than 55 % of the energy supplied by wind and PV, leaving some room for potential improvements. Papadopoulos et al. investigated different scenarios of 15-MW PV in combination with a 1-MW PEM electrolyzer and with or without a battery or a wind turbine [18]. They focused on the utilization factor of the electrolyzer and on the economic feasibility. The utilization factor of the electrolyzer increased from 42 %, for the base case of PV and electrolyzer only, to 66 % when 2 MW of wind power is added to the system and achieves a maximum of 86 %, when a lithium-ion battery with up to 10 MWh is installed. Their economic assessment shows some beneficial cases for battery applications; however, battery investment must not exceed 250 US \$ per kWh. Furthermore, even for high utilization of the electrolyzer, the annual energy used by the electrolyzer is still less than 50 % of the energy provided by wind and PV.

In this work, the combination of an AWE system with a PV power supply is investigated for two exemplary scenarios located in Germany and Morocco. AWE suffers from elevated gas impurities in the part-load range [19–21]. Since PV is not available during the night, PV power needs to be buffered by a battery system. This would allow excess energy during the day to be shifted to the night and the water electrolysis to be operated during the night at a sufficiently high load. A broad variation of AWE power as well as battery power and capacity enables an optimization of all three parameters. Crucial questions that need to be answered are: Firstly, can a battery system buffer the PV output to achieve a high energy usage of the annual PV energy yield, while still ensuring a high operational time of the water electrolyzer with a reasonable capacity (< 20 h of storage at nominal battery load)? Secondly, is there a potential for cost savings by implementation of a well-suited battery?

2 Methodology

The analysis of PV powered water electrolysis is carried out for two scenarios, whereas the first one is located in Morocco and the second one is located in Germany. To analyze a quite realistic scenario, the coordinates of the Quarzazate solar power plant in the region Drâa-Tafilalet of Morocco are applied for the first scenario (31.007° latitude, –6.863° longitude, 1223 m elevation). The coordinates for the site in Germany are corresponding to the PV plant in Pocking, southeast of Bavaria, which is one of the largest PV plants in Germany (48.371° latitude, 13.299° longitude, 325 m elevation).

2.1 Data Basis for the Photovoltaic Power Generation

The Photovoltaic Geographical Information System (PVGIS) of European Commission's science and knowledge service [22] was applied to receive hourly data of power output for a 1 kW_{peak} free-standing, crystalline silicon PV system with optimized slope and azimuth. The total system loss was set to 14 %, which is the default value of the PVGIS tool. Current PV systems might achieve even lower losses in the single digit range; however, we kept the quite high default value in a rather conservative approach. Hourly data for the years 2005 to 2016 was used for the evaluation. In Fig. 1 the power output is visualized as a heat map for the entire time range and the average hourly values over the years are also included. Besides a daily variation a seasonal fluctuation is quite distinct for the Pocking site, while the

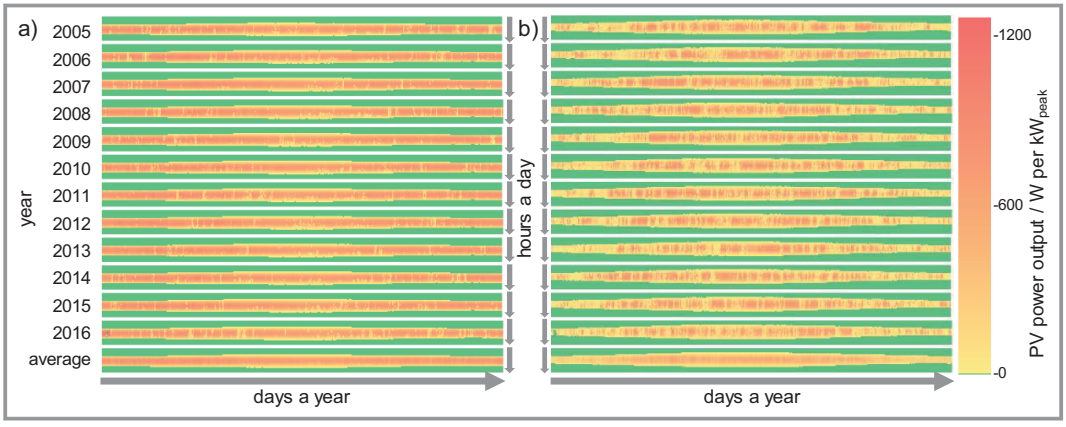

Figure 1. Heat maps visualizing the hourly power output of PV for the two locations under investigation: a) Quarzazate in Morocco, b) Pocking in Germany.

Quarzazate site indicates only almost insignificant seasonal dependence. The annual energy yield is significantly higher in Quarzazate (1907 kWh per kW_{peak}) than the yield in Pocking (1067 kWh per kW_{peak}), which is indicated in more detail in Fig. 2. The specific energy yield is quite narrowly distributed around the maximum power load of 80 % for the Quarzazate location, while the distribution for the Pocking site is much broader with its maximum at 75 % power load.

2.2 Model Setup and Assumptions

The primary target of this evaluation is to find appropriate power and capacity settings to convert as much of the energy provided by the PV system into hydrogen by AWE. To be independent of actual sizes of the system (probably in the range of tens or hundreds of MW), all the values of power or capacity given in this work are referenced to a 1-kW_{peak} PV system. The AWE is capable of following dynamic power load curves [23, 24], however, this applies only if the system and especially the large amount of electrolyte is heated up (approx. 80 °C). In general, a cold start-up procedure with a quick ramp-up of power load is possible, but only at the cost of lower efficiency and potentially enhanced aging of the electrodes. Another limitation affects the hydrogen quality and can be an essential safety issue. If low current densities are applied, i.e., low partial power load, the crossover of hydrogen into the anode chamber and of oxygen into the cathode chamber can cause an exceeding of the lower or upper explosion limit, which would be a severe safety concern. If the partial load is accompanied by shutdown interruptions due to a very high fluctuation of the PV power supply, this risk can become even more severe and appropriate but costly safety routines must be activated.

To circumvent this shutdown and safety issue, a battery could buffer the PV power output enabling a much smoother operation of the AWE above its minimum power load. Fig. 3a describes the scenario without a battery and for an AWE with a maximum power load ($P_{AWE,max}$) lower than the peak power of the PV system ($P_{PV,peak}$). During midday the PV power exceeds the AWE power and part of the energy supplied by the PV system is wasted (or has to be fed into the grid), while at night and at dawn or dusk the PV power is below the minimum power load of the AWE ($P_{AWE,min}$), which in turn leads to wasted energy and shutdown. Fig 3b depicts the same scenario, but at noon the battery stores the excess PV energy that can be released during night at AWE power loads higher than $P_{AWE,min}$. The general setup of the system consisting of PV, battery and AWE is shown Fig. 3c.

The whole data analysis is based on fundamental equations, starting with the energy balance at any timestep t (cf. Eq. (1)).

$$P_{PV}(t) = P_{Batt}(t) + P_{AWE}(t) \tag{1}$$

Here P_{PV}, P_{Batt} and P_{AWE} are the power of the PV system, the battery and the AWE, respectively. The excess power from PV that is exceeding the AWE power range is stored in the battery (if possible), whereas the battery is feeding power to the AWE, if it is sufficiently charged and if the control strategy demands its operation. The capacity C_{Batt} of stored electrical energy in the battery for an exemplary time t_1 is defined by Eq. (2):

$$C_{Batt}(t_1) = -\int_0^{t_1} \frac{P_{Batt}(t)}{1-(1-\eta_{Batt})H(P_{Batt})}\,dt \tag{2}$$

η_{Batt} is the overall efficiency of the battery and H denotes the Heaviside step function, that activates the efficiency

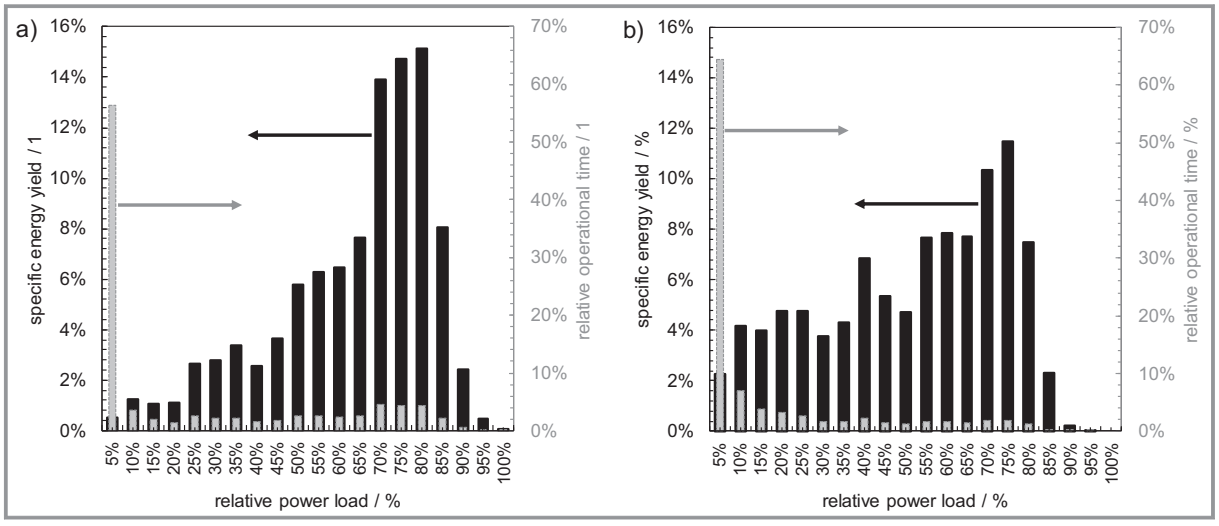

Figure 2. Specific energy yield distribution grouped in 5 % intervals for the two locations under investigation: a) Quarzazate in Morocco, b) Pocking in Germany.

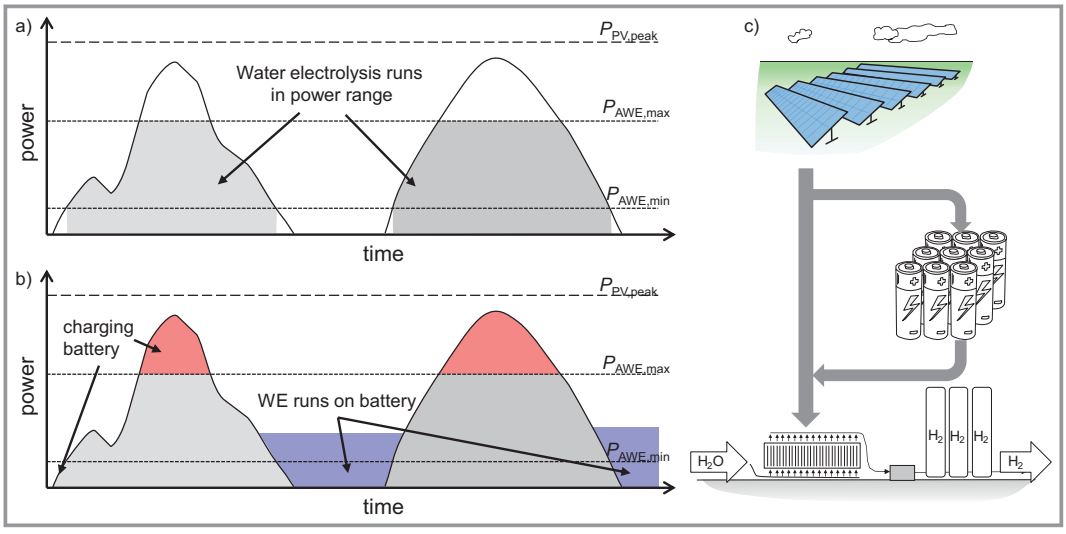

Figure 3. a) Exemplary sketched power output of the PV system for two days with energy usage by the AWE system ($P_{PV,peak}$ = peak power of the PV system, $P_{AWE,max}$ = maximum power of the AWE, $P_{AWE,min}$ = minimum power load of the AWE) and b) resulting load shifting by the battery towards night times. c) System setup of PV, battery and AWE.

only during discharge, since for simplicity we assume that all losses within the battery are virtually summed up in the discharge process. However, to simplify the evaluation even further an overall battery efficiency of 100 % is assumed. This assumption is certainly not valid for real battery systems (redox flow battery systems might achieve 70 % round trip system efficiency, while Li-battery system can reach up to approximately 90 % round trip efficiency depending on load profile [25]). Nevertheless, to investigate the principal behavior of the combination of a battery (or an equivalent energy storage system) with a PV system and an AWE, this assumption helps to identify the theoretical optimum. Therefore, a more detailed analysis covering the aspect of load-dependent efficiency might be more appropriate as a next step. Accordingly, the efficiency of water electrolysis is assumed to be 100 % as well, which again is not a realistic assumption. The overall efficiency of a water electrolysis system is in the range of approx. 75 % depending on power load. The variation of efficiency as a function of power load is governed by the quite constant losses of the system equipment (pumps, instrumentation, process control system) and power-dependent losses due to overvoltages within each cell of the electrolyzer. Both terms compensate in a way that only a decent dependency on power load in a range of 70 % to 80 % is expectable. Hence, assuming a water electrolysis efficiency of 100 % leads to a value that does not exactly correspond to the amount of hydrogen produced, but rather to the amount of electrical energy fed into the water electrolyzer.

The hourly power output of the PV system P_{PV} is given by the PVGIS database and referred to a 1-kW_{peak} system. The power range of the water electrolyzer lies within its maximum and minimum power loads $P_{AWE,min}$, $P_{AWE,max}$, respectively:

$$0 < P_{AWE,min} < P_{AWE}(t) < P_{AWE,max} \quad (3)$$

The possible power range of the battery is limited by its maximum power load $P_{Batt,max}$, which is assumed to be valid for charging and discharging of the battery and current and maximum capacity, $C_{Batt}(t)$ and $C_{Batt,max}$, respectively:

$$\max\left(\frac{-\left(C_{Batt,max} - C_{Batt}(t)\right)}{1\ h}; -P_{Batt,max}\right) < P_{Batt}(t) < \min\left(\frac{C_{batt}(t)}{1\ h}; P_{Batt,max}\right) \quad (4)$$

The power control of the battery and electrolyzer is set up in the following way. The main priority is the operation of the AWE, therefore all the power of the PV is fed into the electrolyzer, while the PV power output is above the minimum and below the maximum power of the water electrolyzer system. If the PV power exceeds the maximum water electrolyzer power limit, the excess energy is fed into the battery until the battery is fully charged. If the PV power system falls below $P_{AWE,min}$, the battery delivers as much additional power to maintain the operation of the water electrolyzer at $P_{AWE,min}$ until the battery is discharged. This is defined as control strategy "static min". A second control strategy, defined "dynamic min", differs in that the minimum power fed into the electrolyzer is dynamically adapted to the average PV power output of the next 48 h, if this value is not exceeding battery or electrolyzer power limits. The implementation of these two described control strategies and the corresponding equations can be found in detail in the Supporting Information (SI). The first strategy ensures to operate the water electrolyzer as long as possible during times of low PV energy yield, while it leads to potential

waste of PV energy, if the energy stored during daytime cannot be used completely in the electrolyzer during nighttime. The second control strategy aims at the reduction of this waste of PV energy, since it improves the match between PV energy yield, mostly during daytime and the continuous energy usage in the electrolyzer on a daily basis. Therefore, the probable minimum time interval should be 24 h, but 48 h were chosen to avoid electrolysis downtime, due to potentially significant changes of the daily PV energy yield (e.g., one cloudy day in the summer). Longer time intervals were not chosen, due the assumption of a good weather forecast and therefore good PV power forecast only for the next 48 h. Of course, more advanced process control would be necessary for real operation, using professional weather and power forecasts combined with appropriate control algorithms for acceptable probabilities of shutdown time and energy wasting. However, the two control strategies presented in this work, are easy to understand and can help to visualize the effects of different control settings.

To investigate the effect of different power settings following variations are applied: The water electrolyzer power is varied in steps of 50 W per kW_{peak} up to 1000 W per kW_{peak}. The maximum battery power is varied in steps of 100 W per kW_{peak} up to 1000 W per kW_{peak} and the battery capacity is varied in steps of 0.5 h up to 20 h storage time at maximum load. All these variations are carried out for the indicated two locations and for two control strategies of battery discharge power. The minimum AWE power limit is assumed to be at 20 % of the maximum power load and the data is evaluated on an hourly basis for the years 2005 to 2016. Due to the simplicity of the model, the evaluation could be carried out using Microsoft Excel® and the applied datasheet can be found in the SI.

The output of the parameter variation can be evaluated by using two important target parameters. The first is defined as renewable energy usage ε, which is determined by the amount of energy fed into the water electrolyzer related to the total yield of PV energy over the whole dataset (for $0 < t < t_{max}$):

$$\varepsilon = \frac{\int_0^{t_{max}} P_{AWE}(t)\mathrm{d}t}{\int_0^{t_{max}} P_{PV}(t)\mathrm{d}t} \tag{5}$$

The second is the time usage τ, which defines the operation time of the water electrolyzer compared to the entire time of the dataset:

$$\tau = \frac{\int_0^{t_{max}} H(P_{AWE})\mathrm{d}t}{t_{max}} \tag{6}$$

A third parameter time*energy usage λ is quite artificially defined as the product of energy usage and time usage:

$$\lambda = \varepsilon\tau \tag{7}$$

3 Results and Discussion

The two target parameters renewable energy usage and time usage are applied for the evaluation of the parameter variation of the scenarios, as described in the previous section. In Fig. 4 these two parameters are presented for the scenario in Morocco and the control strategy "dynamic min" for the whole power and capacity variation. As a base case the target parameters are given for a scenario without battery usage ($P_{Batt,max} = 0$). For this case, it is apparent that the energy usage increases steadily with increasing AWE power until it reaches a quite constant level of 95 %. This behavior is expectable, since an increased AWE power reduces the time, during which PV power output exceeds the maximum AWE power limit. However, an increase of the AWE power also reduces the time usage from approximately 45 % to 40 % (cf. Fig 4b), which can be explained by the fixed ratio of minimum and maximum AWE power, leading to more

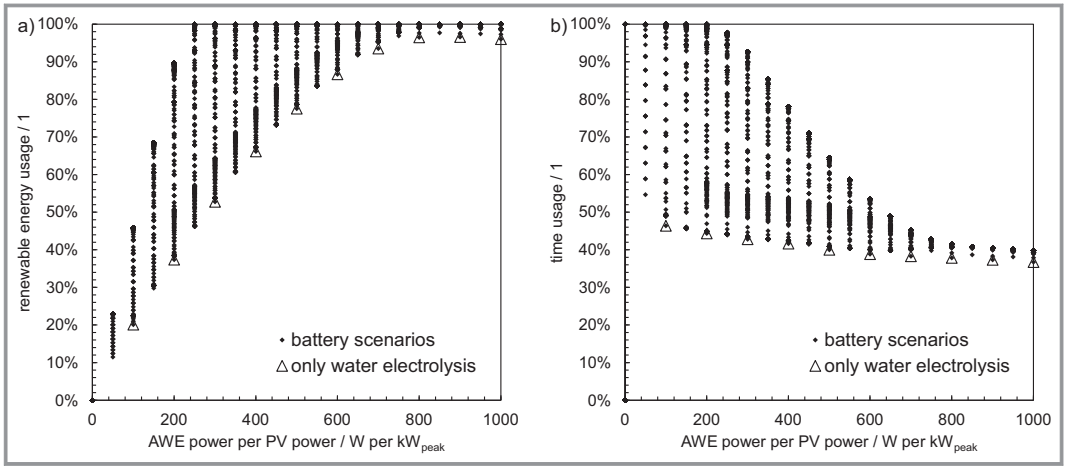

Figure 4. Model results for the two target parameters renewable energy usage (a) and time usage (b) for the Quarzazate location using the "dynamic min" control strategy. All parameter variations are compared to scenarios without battery usage.

incidences of PV power output being lower than the minimum AWE power, and thus a lowered operating time.

When considering all the battery cases as well, it is obvious that an increase of both target parameters up to 100 % can be achieved. The energy usage reaches up to 100 % for an AWE power of more than 200 W per kW_{peak} (cf. Fig 4 a). If one takes into account that the annual energy yield in Morocco of 1907 kWh per kW_{peak} can be converted into a constant average PV power output of 218 W per kW_{peak} this result is clear and the PV power fluctuations just need to be buffered by appropriate battery settings. Higher levels of the AWE power lead to less battery charging during daytime and thus a lower battery capacity available for discharging at night. This results in a higher number of shutdowns during the night and a lowered time usage.

The enveloped curve of maximum achievable renewable energy usages is visualized in Fig. 5. Both control strategies increase the energy usage, whereas the "dynamic min" strategy outperforms the "static min" strategy. As already mentioned, the "static min" strategy can lead to increased wasting of energy, thus lowering the maximum achievable energy usage. A comparison of the two locations in Morocco and Germany under the "dynamic min" control strategy indicates a difference when a sufficient maximum AWE power leads to the maximum level of energy usage. For the Morocco case, an AWE power of 250 W per kW_{peak}, which is just close above the annual average PV power output (218 W per kW_{peak}), guarantees a high energy usage ratio (cf. Fig. 5a). In Germany instead, the maximum AWE power has to be 200 W per kW_{peak} to achieve the highest level of energy usage, although the annual average PV power output is only 122 W per kW_{peak}. This is probably a result of the higher seasonal fluctuation of PV power in Germany, thus a higher AWE power than the annual average PV power must be provided in the summer season. Otherwise, the battery capacity would have to be extraordinarily large to buffer seasonal fluctuation as well, which is very unlikely to be an economically and technically feasible alternative.

The maximum values for the time usage are depicted in Fig. 6. It is evident that a low AWE power level can lead up to 100 % time usage, when the AWE power is below or only slightly larger than the annual average PV power. This is easily explained by the lower level of minimum power for the AWE, which can be provided by the PV even during days of low solar irradiation. Especially for the Morocco location a significant difference is apparent for the two different control strategies and as the "static min" strategy is setting a higher priority to longer discharge durations. It is clear that this strategy allows a higher time usage ratio even for AWE power ranges distinctly above the annual average PV power. However, for increasing power levels of the AWE up to 700 to 1000 W per kW_{peak}, the battery is unable to improve the time usage significantly, due to the low remaining battery charging power at midday.

Since an optimal design of AWE power as well as battery power and capacity would rely on high values for energy usage and time usage, both parameters can be combined by simply calculating the product of both. This combined target parameter is defined as time*energy usage, the dependence of which on AWE power is depicted in Fig. 7. The evaluation for the scenario in Morocco indicates a high time*energy usage that is achievable for an AWE power slightly higher than the annual average PV power for the dynamic min control strategy and distinctly higher for the static min control strategy. The achievable values for the location in Germany are somewhat lower, but nevertheless, clear optima are resulting for all four scenarios. Several corresponding sets of battery power and battery capacity parameters exist, and it is of major interest to identify the lowest battery power and capacity values that still maintain a high value of the target parameter. To identify these lowest values for battery power and capacity, a bandwidth of 98 % to 100 % of congruence to the overall target parameter

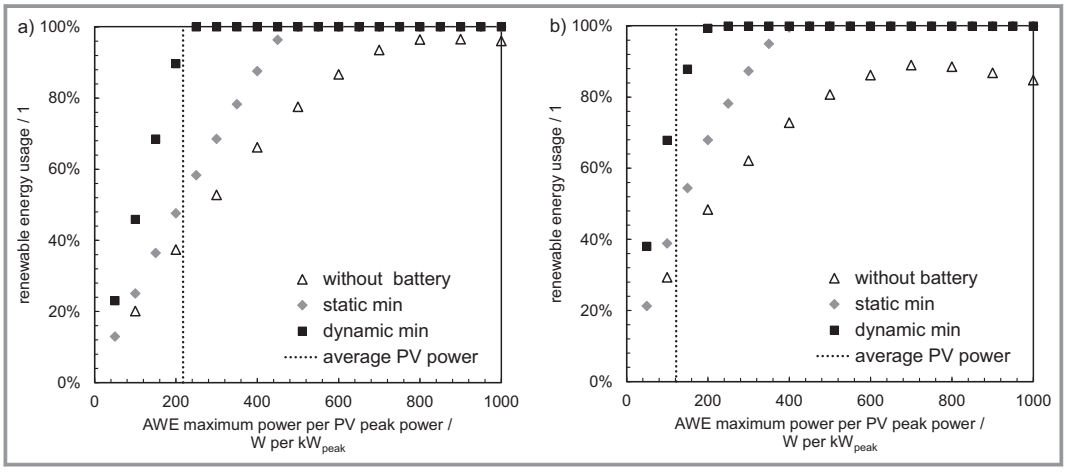

Figure 5. Maximum of achievable energy usages for the Quarzazate scenario (a) and for the Pocking scenario (b) under different control strategies and compared to the base case without battery.

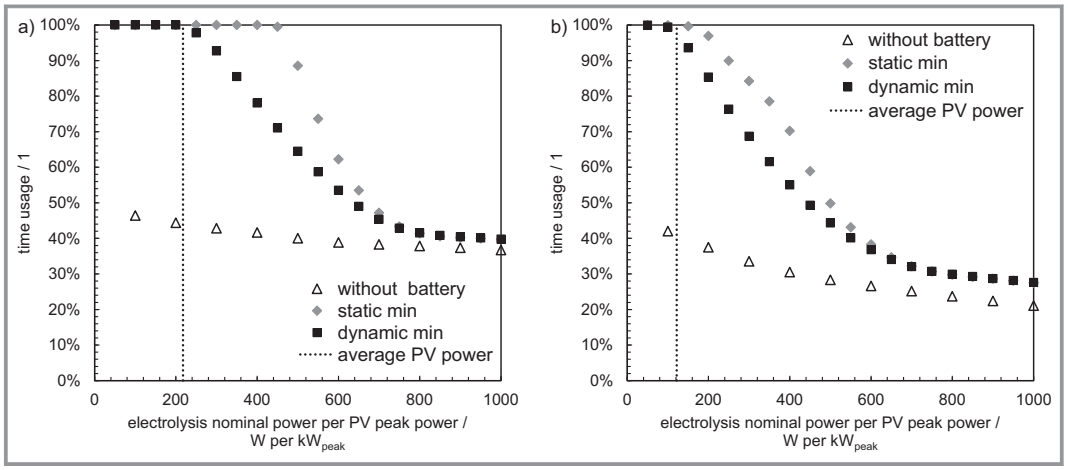

Figure 6. Maximum of achievable time usage for the Quarzazate scenario (a) and for the Pocking scenario (b) under different control strategies and compared to the base case without battery.

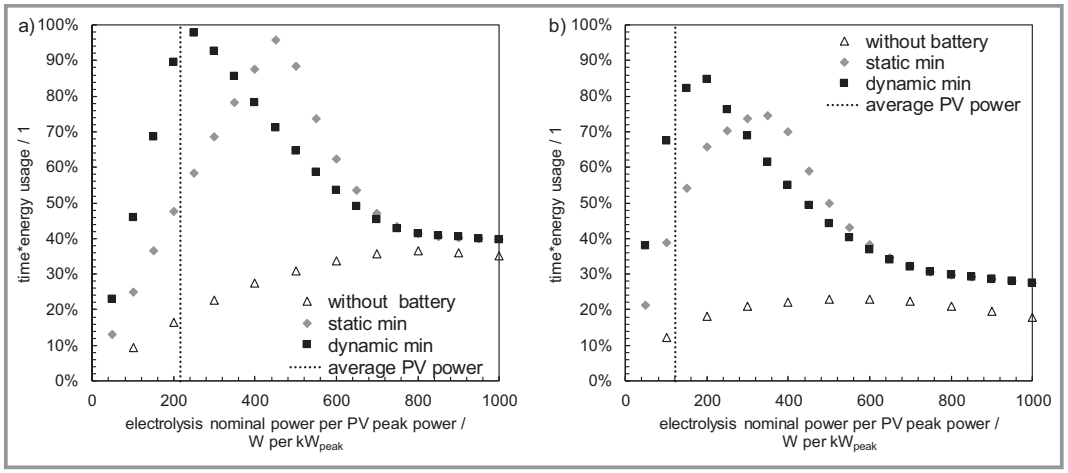

Figure 7. Maximum of achievable combined time*energy usages for the Quarzazate scenario (a) and for the Pocking scenario (b) under different control strategies and compared to the base case without battery.

optimum is applied and within this bandwidth the lowest battery power combined with its corresponding lowest battery capacity is selected. The resulting target parameters and corresponding power and capacity settings are summarized in Tab. 1.

The data in Tab. 1 indicates that for all four optimum cases the corresponding battery capacity exceeds a value of 4 h and especially for the Pocking scenario under "dynamic min" control strategy a very high battery capacity of 17 h is required. For the other scenarios more realistic, but still quite high, capacities of at least 5 h are necessary. The required AWE power indicated in Tab. 1 ranges from 200 to 450 W per kW$_{peak}$. This corresponds to a very significant decrease of required AWE

Table 1. Corresponding power and capacity design for AWE and battery at the optima for all four scenarios.

	Quarzazate		Pocking	
Control strategy [–]	static min	dynamic min	static min	dynamic min
Energy usage [%]	96	100	95	99
Time usage [%]	99	98	79	85
Time*energy usage [%]	96	98	75	85
AWE power [W kW$_{peak}^{-1}$]	450	250	350	200
Min. battery power [W kW$_{peak}^{-1}$]	300	500	350	500
Min. battery capacity [h] [a)]	5	7	5	17
Min. battery capacity [kWh kW$_{peak}^{-1}$]	1.5	3.5	1.75	8.5

a) Maximum discharge time at maximum power load of the battery.

;power when it is compared to the scenarios with high energy yields without battery application (cf. Fig. 5). The maximum energy yield for the Quarzazate location without a battery is 97 % achieved for an AWE power of 900 W per kW_{peak} and 89 % at 700 W per kW_{peak} for the Pocking location, respectively. The reduction of required AWE power can be converted into costs savings if we asses appropriate CAPEX costs for the AWE. The power specific costs of AWE lie in the range of 500 $ to 1000 $ per kW, so we may assume 750 $ per kW [26–28]. Therefore, cost savings of approximately 260 $ to 490 $ per kW_{peak} are possible. However, these savings have to be related to the necessary battery capacity for the corresponding optimized scenario to enable a comparison to available literature data for battery costs. The results are presented in Tab. 2 and the range of maximum capacity specific battery costs is between 44 and 225 $ per kWh. This break-even point for economic feasibility is challenging, since large-scale battery energy storage achieved costs of 393 $ to 581 $ per kWh in 2018 [25]. The future development of this break-even point is of course significantly affected by cost reductions of water electrolysis and battery storage. Thus, the combination of PV with battery and AWE might become economically feasible if battery costs decrease substantially faster than the costs for water electrolysis.

Table 2. Potentials for AWE power reduction and resulting cost savings for the comparison of optimized scenarios with and without a battery.

	Quarzazate		Pocking	
Control strategy [–]	static min	dynamic min	static min	dynamic min
AWE power w/o battery [W kW_{peak}^{-1}]	900	900	700	700
Energy usage w/o battery [%]	97%	97%	89%	89%
AWE power reduction [W kW_{peak}^{-1}]	450	650	350	500
AWE power specific costs [$ kW^{-1}]	750	750	750	750
AWE cost reduction [$ kW_{peak}^{-1}]	337,5	487,5	262,5	375
Break even battery costs [$ kWh^{-1}]	225	139	150	44

Although this cost estimation does not show an economic feasibility yet, it is important to consider the technological advantages of increased energy usage, reduced shutdown time, reduced heat up procedures and lower risk of gas impurities for a combined AWE and battery system. Furthermore, potential costs reductions could be possible by improved control strategies and costs sensitive system design optimizations.

4 Conclusion

Water electrolysis powered by PV is an essential combination for the decarbonization of our economy. The additional application of a battery can reduce the required power of an AWE and can increase the energy usage and time usage. The effect of a control strategy on the target parameters is less pronounced for the Morocco site than for the Germany site. Therefore, the AWE power reduction at the Morocco site is higher for the dynamic min strategy compared to the static min strategy and the Germany site, respectively. Thus, an increase of both parameters is achievable for appropriately optimized AWE and battery power as well as battery capacity. Depending on the location and the control strategy for optimized setups, the battery power is equal or greater than the AWE power and the battery capacity is always greater than 5 h.

Although the optimized setup does not seem to achieve economic feasibility, this can be within reach for ongoing cost reductions in battery technologies. Considering additional optimization of the control strategy and a system setup that focuses more on achievable cost savings, it should be possible to identify economically attractive solutions. Further improvements can be made when investigating other locations, adding wind power to the system, applying other forms of solar power and energy storage (maybe concentrated solar power with thermal energy storage as already applied in Quarzazate) and when the future cost development of water electrolysis and battery energy storage can be estimated more precisely.

Besides cost savings the battery allows a continuous operation of the AWE, mitigating safety issues of crossover of hydrogen and oxygen, at least for the Morocco location. The seasonal fluctuation in Germany does not allow usage all time. Nevertheless, a seasonal production of hydrogen in Germany in the summer season would still benefit from the battery's buffering behavior. During winter season the battery might not buffer the hydrogen production, but other services such as power reserve and grid stabilization are additional opportunities.

Supporting Information

Supporting Information for this article can be found under DOI: 10.1002/cite.202000151. This section includes the Excel files applied for the data analysis.

The authors gratefully acknowledge the funding of the Deutsche Forschungsgemeinschaft (DFG, German Research Foundation) project numbers: 290019031; 391348959. Open Access funding enabled and organized by Projekt DEAL.

Symbols used

C	[Wh]	capacity
P	[W]	power
ε	[–]	energy usage
λ	[–]	time*energy usage
τ	[–]	time usage

Sub- and Superscripts

AWE,min	alkaline water electrolysis minimum power
AWE,max	alkaline water electrolysis maximum power
Batt,max	battery maximum power or capacity

Abbreviations

AWE	alkaline water electrolysis
Batt	battery
PV	photovoltaics

References

[1] M. Allen et al., *Summary for Policymakers*, in *Global Warming of 1.5°C. An IPCC Special Report on the impacts of global warming of 1.5°C above pre-industrial levels and related global greenhouse gas emission pathways, in the context of strengthening the global response to the threat of climate change, sustainable development, and efforts to eradicate poverty* (Eds: V. Masson-Delmotte et al.), IPCC, Geneva **2018**.

[2] *A hydrogen strategy for a climate-neutral Europe*, European Commission, Brussels **2020**.

[3] *Die Nationale Wasserstoffstrategie*, Bundesregierung Deutschland, Berlin **2020**.

[4] *Norddeutsche Wasserstoff Strategie*, Wirtschafts- und Verkehrsministerien der norddeutschen Küstenländer, **2019**.

[5] www.rechargenews.com/transition/solar-hits-new-record-low-with-14-80-mwh-winning-bid-in-portugal/2-1-647124 (accessed on December 27, 2020)

[6] https://cleantechnica.com/2019/09/23/uk-offshore-wind-prices-reach-new-record-low-in-latest-cfd-auction/ (accessed on December 27, 2020)

[7] www.greentechmedia.com/articles/read/mexico-auction-bids-lowest-solar-wind-price-on-the-planet (accessed on December 27, 2020)

[8] H. Dagdougui, A. Ouammi, C. Bersani, R. Sacile, *Hydrogen infrastructure for energy applications: Production, storage, distribution and safety*, Academic Press, London **2018**.

[9] M. Schalenbach et al., *Int. J. Electrochem. Sci.* **2018**, *13*, 1173–1226. DOI: https://doi.org/10.20964/2018.02.26

[10] M. Carmo, D. L. Fritz, J. Mergel, D. Stolten, *Int. J. Hydrogen Energy* **2013**, *38 (12)*, 4901–4934. DOI: https://doi.org/10.1016/j.ijhydene.2013.01.151

[11] A. Khalilnejad, G. H. Riahy, *Energy Convers. Manage.* **2014**, *80*, 398–406. DOI: https://doi.org/10.1016/j.enconman.2014.01.040

[12] P. Hou, P. Enevoldsen, J. Eichman, W. Hu, M. Z. Jacobson, Z. Chen, *J. Power Sources* **2017**, *359*, 186–197. DOI: https://doi.org/10.1016/j.jpowsour.2017.05.048

[13] M. Gökçek, C. Kale, *Int. J. Hydrogen Energy* **2018**, *43 (23)*, 10615–10625. DOI: https://doi.org/10.1016/j.ijhydene.2018.01.082

[14] A. Al-Sharafi, A. Z. Sahin, T. Ayar, B. S. Yilbas, *Renewable Sustainable Energy Rev.* **2017**, *69*, 33–49. DOI: https://doi.org/10.1016/j.rser.2016.11.157

[15] S. H. Siyal, D. Mentis, M. Howells, *Int. J. Hydrogen Energy* **2015**, *40 (32)*, 9855–9865. DOI: https://doi.org/10.1016/j.ijhydene.2015.05.021

[16] J. Brauns, T. Turek, *Processes* **2020**, *8 (2)*, 248. DOI: https://doi.org/10.3390/pr8020248

[17] O. Machhammer, C. Henschel, *Chem. Ing. Tech.* **2021**, *93 (4)*, in press. DOI: https://doi.org/10.1002/cite.202000153

[18] V. Papadopoulos, J. Desmet, J. Knockaert, C. Develder, *Int. J. Hydrogen Energy* **2018**, *43 (34)*, 16468–16478. DOI: https://doi.org/10.1016/j.ijhydene.2018.07.069

[19] P. Haug, M. Koj, T. Turek, *Int. J. Hydrogen Energy* **2017**, *42 (15)*, 9406–9418. DOI: https://doi.org/10.1016/j.ijhydene.2016.12.111

[20] P. Haug, B. Kreitz, M. Koj, T. Turek, *Int. J. Hydrogen Energy* **2017**, *42 (24)*, 15689–15707. DOI: https://doi.org/10.1016/j.ijhydene.2017.05.031

[21] P. Trinke, P. Haug, J. Brauns, B. Bensmann, R. Hanke-Rauschenbach, T. Turek, *J. Electrochem. Soc.* **2018**, *165 (7)*, F502–F513. DOI: https://doi.org/10.1149/2.0541807jes

[22] https://re.jrc.ec.europa.eu/pvg_tools/en/#PVP (accessed on December 27, 2020)

[23] W. Hug, J. Divisek, J. Mergel, W. Seeger, H. Steeb, *Int. J. Hydrogen Energy* **1992**, *17 (9)*, 699–705. DOI: https://doi.org/10.1016/0360-3199(92)90090-J

[24] W. Hug, H. Bussmann, A. Brinner, *Int. J. Hydrogen Energy* **1993**, *18 (12)*, 973–977. DOI: https://doi.org/10.1016/0360-3199(93)90078-O

[25] K. Mongird, V. Fotedar, V. Viswanathan, V. Koritarov, P. Balducci, B. Hadjerioua, J. Alam, *Energy Storage Technology and Cost Characterization Report*, U.S. Department of Energy, Washington, DC **2019**.

[26] O. Schmidt, A. Gambhir, I. Staffell, A. Hawkes, J. Nelson, S. Few, *Int. J. Hydrogen Energy* **2017**, *42 (52)*, 30470–30492. DOI: https://doi.org/10.1016/j.ijhydene.2017.10.045

[27] J. Proost, *Int. J. Hydrogen Energy* **2019**, *44 (9)*, 4406–4413. DOI: https://doi.org/10.1016/j.ijhydene.2018.07.164

[28] S. M. Saba, M. Müller, M. Robinius, D. Stolten, *Int. J. Hydrogen Energy* **2018**, *43 (3)*, 1209–1223. DOI: https://doi.org/10.1016/j.ijhydene.2017.11.115

